Pharm Res (2013) 30:1999–2009
DOI 10.1007/s11095-013-1044-1

RESEARCH PAPER

Trastuzumab Labeled to High Specific Activity with ^{111}In by Conjugation to G4 PAMAM Dendrimers Derivatized with Multiple DTPA Chelators Exhibits Increased Cytotoxic Potency on HER2-Positive Breast Cancer Cells

Conrad Chan • Zhongli Cai • Raymond M. Reilly

Received: 5 January 2013 / Accepted: 1 April 2013 / Published online: 25 April 2013

ABSTRACT

Purpose To conjugate trastuzumab with/without NLS peptides to G4 PAMAM dendrimers derivatized with DTPA and determine the specific radioactivity (SA) for ^{111}In labeling, HER2 immunoreactivity and cytotoxicity on breast cancer (BC) cells.

Methods G4 dendrimers were reacted with DTPA then conjugated through a thiol to maleimide-derivatized trastuzumab. The SA achievable was determined by incubating 2 to 20 μg with 60 MBq of ^{111}In. HER2 immunoreactivity, internalization and nuclear importation were measured. The effect of ^{111}In-DTPA-G4-trastuzumab (5.9 MBq/μg) on the clonogenic survival (CS) of SK-Br-3 or MDA-MB-231 cells with high or low HER2 density, respectively was compared to ^{111}In-DTPA-NLS-trastuzumab (0.5 MBq/μg). DNA double-strand breaks (DSBs) were measured.

Results DTPA-G4-trastuzumab was labeled with ^{111}In to a SA (23.6 MBq/μg) which was 100-fold higher than ^{111}In-DTPA-NLS-trastuzumab. ^{111}In-DTPA-G4-trastuzumab and ^{111}In-DTPA-G4-NLS-trastuzumab retained HER2 immunoreactivity and were internalized and imported into the nucleus of BC cells. G4-radioimmunoconjugates were 2–4 fold and 9-fold more cytotoxic to SK-Br-3 and MDA-MB-231 cells, respectively than ^{111}In-DTPA-NLS-trastuzumab which was associated with an increase in DNA DSBs.

Conclusions Conjugation of trastuzumab to G4 PAMAM dendrimers modified with 30 DTPA permitted high SA ^{111}In labeling which increased their cytotoxic potency for BC cells with high or low HER2 density.

KEY WORDS Breast cancer · HER2 · Indium-111 · PAMAM dendrimers · Trastuzumab

ABBREVIATIONS

γ-H2AX	gamma-histone 2AX
BC	breast cancer
BSA	bovine serum albumin
CS	clonogenic survival
DSBs	double-strand breaks
DTPA	diethylenetriaminepentaacetic acid
EC_{50}	effective concentration-50%
FBS	fetal bovine serum
G4	generation 4
HER2	human epidermal growth factor receptor-2
IB4M	2-(para-isothiocyanatobenzyl)-6-methyl-DTPS
ITLC-SG	instant thin layer-silica gel chromatography
LET	linear energy transfer
M_r	molecular weight
MWCO	molecular weight cut-off
NLS	nuclear translocation sequence
PAMAM	polyamidoamine
PBS	phosphate-buffered saline
RT	room temperature
SA	specific radioactivity
sulfo-SMCC	sulfosuccinimidyl-4-(*N*-maleimidomethyl)cyclohexane-1-carboxylate
SV40	Simian virus 40

C. Chan · Z. Cai · R. M. Reilly (✉)
Department of Pharmaceutical Sciences, University of Toronto
144 College St. Toronto, Ontario, Canada M5S 3M2
e-mail: raymond.reilly@utoronto.ca

R. M. Reilly
Department of Medical Imaging, University of Toronto
Toronto, Ontario, Canada M5S 3E2

R. M. Reilly
Toronto General Research Institute, University Health Network
Toronto, Ontario, Canada M5G 2C4

INTRODUCTION

The human epidermal growth factor receptor-2 (HER2) is overexpressed due to gene amplification in 15–30% of breast cancers (BC) (1) and is the target for treatment with trastuzumab (Herceptin) used as a single agent (2) or combined with chemotherapy (*e.g.* anthracyclines or paclitaxel) (3). Nonetheless, only 12–35% of patients with metastatic HER2-positive BC responded to trastuzumab monotherapy in Phase 2 clinical trials while 50% responded when trastuzumab was combined with anthracyclines in randomised Phase 3 trials (3–5). In order to increase its effectiveness, our group has modified trastuzumab with diethylenetriaminepentaacetic acid (DTPA) for complexing the Auger-electron emitting radionuclide ^{111}In (6). The very low energy (<25 keV) Auger electrons emitted by ^{111}In have high linear energy transfer (LET) since they deposit their energy within nanometer-micrometer distances. Thus, decay of ^{111}In in close proximity or in the nucleus of BC cells causes extensive DNA double-strand breaks (DSBs) resulting in cell death (7). A nuclear translocation sequence (NLS) peptide [CGYGPKKKRKVGG] containing a short sequence of cationic residues (underlined) from the simian virus 40 (SV40) large T-antigen (8) was conjugated to ^{111}In-DTPA-trastuzumab to route these radioimmunoconjugates to the nucleus of BC cells (6). ^{111}In-DTPA-NLS-trastuzumab was 2–5 fold more cytotoxic *in vitro* than ^{111}In-DTPA-trastuzumab without NLS on SK-Br-3 human BC cells with high HER2 expression (1.3×10^6 receptors/cell) and 3 to 6-fold more potent than unlabeled trastuzumab. However, ^{111}In-DTPA-NLS-trastuzumab was less potent for killing MDA-MB-361 BC cells with moderate HER2 density (5.1×10^5 receptors/cell) with only 1.3–2 fold greater cytotoxicity than ^{111}In-DTPA-trastuzumab. MDA-MB-231 cells with low HER2 density (5.4×10^4 receptors/cell) were resistant. Treatment of athymic mice implanted s.c. with MDA-MB-361 tumor xenografts with moderate HER2 density with a single dose of ^{111}In-DTPA-NLS-trastuzumab (9.25 MBq; 4 mg/kg) showed 2.3-fold significantly greater reduction in tumor growth rate than in mice treated with ^{111}In-DTPA-trastuzumab and 3.3-fold greater reduction in tumor growth rate than unlabeled trastuzumab. However, no tumor growth inhibitory effects were found for MDA-MB-231 xenografts that have low HER2 density (9).

Our aim in the current study was to increase the cytotoxic potency of ^{111}In-DTPA-NLS-trastuzumab, especially for BC cells with low-moderate HER2 density since patients with tumors with these characteristics are not eligible for trastuzumab (Herceptin) treatment (10). One strategy to increase the potency would be to increase the specific radioactivity (SA) in order to maximize the amount of ^{111}In deposited in HER2-positive tumor cells per receptor recognition event. At the SA previously achieved for ^{111}In-DTPA-NLS-trastuzumab (<0.24 MBq/μg; $<3.6\times10^4$ MBq/μmole), only 1 in 50 molecules was radiolabeled. Thus, a high proportion of HER2 were bound by non-radiolabeled immunoconjugates, limiting the cytotoxic potency. Increasing the DTPA substitution level of trastuzumab to increase the SA may not be feasible, since the immunoreactivity of antibodies is often compromised if too many metal chelators are conjugated (11). In an earlier report, we described conjugation of trastuzumab Fab fragments to metal-chelating polymers which increased the SA for ^{111}In labeling by up to 100-fold compared to DTPA-trastuzumab Fab (12). An alternative strategy is to append polyamidoamine (PAMAM) dendrimers modified with multiple DTPA chelators for ^{111}In to trastuzumab which have been shown to increase the delivery of therapeutic agents and radionuclides to tumors (13–15). The 64 surface reactive amino groups on generation 4 (G4) PAMAM dendrimers were derivatized with multiple DTPA chelators and conjugated to trastuzumab with or without NLS-peptide modification for high SA labeling with ^{111}In. The internalization and nuclear importation properties of these G4 radioimmunoconjugates were examined since these are important for the cytotoxicity of the ultrashort-range Auger electrons (16). Finally, the ability of high SA G4-radioimmunoconjugates to cause DNA DSBs and decrease the clonogenic survival (CS) of SK-Br-3 cells with high HER2 density or MDA-MB-231 cells with low HER2 density were compared to low SA ^{111}In-DTPA-NLS-trastuzumab.

MATERIALS AND METHODS

Cell Culture

SK-Br-3 and MDA-MB-231 human BC cells were obtained from the American Type Culture Collection (Manassas, VA). SK-Br-3 cells were cultured in RPMI 1640 medium with 10% fetal bovine serum (FBS), 5% CO_2. MDA-MB-231 cells were maintained in Dulbecco's modified Eagle medium with 10% FBS and 1% Penicillin-Streptomycin. The HER2 density of SK-Br-3 and MDA-MB-231 cells is 1.3×10^6 and 5.4×10^4 receptors per cell, respectively (17).

DTPA-G4-Trastuzumab Immunoconjugates

G4 PAMAM dendrimer was derivatized with DTPA as described by Kobayashi H. *et al.* (18) with some modifications (Fig. 1). Briefly, 14.2 kDa G4 PAMAM dendrimers (Sigma-Aldrich, St. Louis, MO) were reacted with a 500:1 mole excess of DTPA dianhydride (Sigma-Aldrich) in 0.5 M NaH_2PO_4 buffer, pH 9.0 at 40°C for 18 h. DTPA-G4 was purified from excess DTPA and exchanged into 0.5 M

NaH_2PO_4 buffer, pH 8.0 by ultrafiltration on an Amicon Ultra-3 K (molecular weight cut-off, MWCO = 3 kDa) device (Millipore, Billerica, MA). To introduce thiol groups into G4-DTPA, the remaining primary amine groups were reacted with a 5:1 mole excess of 2-iminothiolane (Traut's reagent, Pierce Chemical Co., Rockford, IL) in 0.5 M NaH_2PO_4 buffer, pH 8.0 for 1 h at room temperature (RT) under N_2. Thiolated G4-DTPA was purified and buffer exchanged into phosphate buffered saline (PBS), pH 7.0 by ultrafiltration on an Amicon Ultra-3 K device. Maleimide groups were introduced into trastuzumab (Herceptin, Hoffman-La Roche, Mississauga, ON; 3–5 mg/mL) by reaction with a 10:1 mole excess of sulfo-SMCC (5 mmol/L, Pierce) in PBS pH 7.6 at RT for 1 h, then purified and buffer-exchanged into PBS, pH 7.0, on a Amicon Ultra-30 K device (MWCO = 30 kDa). Maleimide-derivatized trastuzumab was reacted with thiolated G4-DTPA at a 1:12 mole ratio in PBS, pH 7.0 at 30°C for 18 h. Finally, DTPA-G4-trastuzumab was purified from excess thiolated G4-DTPA on an Amicon Ultra-100 K (MWCO 100 kDa) device.

DTPA-G4-NLS-Trastuzumab Immunoconjugates

Modification of DTPA-G4-trastuzumab with NLS peptides was performed as reported (6). Briefly, DTPA-G4-trastuzumab in PBS, pH 7.6, was reacted with a 10-fold mole excess of sulfosuccinimidyl-4-(*N*-maleimidomethyl)cyclohexane-1-carboxylate (sulfo-SMCC; 5 mmol/L) at RT for 1 h, then purified and buffer-exchanged into PBS, pH 7.0 on an Amicon Ultra-30 K device (Fig. 1). Purified maleimide-derivatized DTPA-G4-trastuzumab was reacted with a 50-fold mole excess of NLS peptides (CGYGPKKKRKVGG; Advanced Protein Technology Centre, The Hospital for Sick Children, Toronto, ON) in 10 mmol/L PBS, pH 7.0 for 18 h at 4°C. Finally, DTPA-G4-NLS-trastuzumab was purified on an Amicon Ultra-30 K device. Irrelevant non-specific human IgG (Sigma-Aldrich) was similarly conjugated to DTPA-G4 and NLS peptides. DTPA-NLS-trastuzumab without G4 was constructed as previously reported (6).

Purity and Homogeneity of Immunoconjugates

The purity and homogeneity of DTPA-NLS-trastuzumab, DTPA-G4-trastuzumab or DTPA-G4-NLS-trastuzumab were evaluated by SDS-PAGE analysis under non-reducing conditions on 5% Tris–HCl mini-gel (BioRad, Mississauga, ON) stained with Coomassie brilliant blue. The number of G4-DTPA groups and NLS peptides conjugated to trastuzumab was estimated from the upward shift in the IgG band on the gel associated with an increase in the molecular weight (M_r) resulting from these modifications. Conjugation of trastuzumab to each G4 dendrimer modified with 30 DTPA results in a 26 kDa increase in the M_r of trastuzumab while each NLS peptide conjugation yields an increase of 1.85 kDa.

Radiolabeling of Immunoconjugates

DTPA-G4-trastuzumab, DTPA-G4-NLS-trastuzumab, DTPA-NLS-trastuzumab or DTPA-G4-NLS-IgG were radiolabeled by incubation with $^{111}InCl_3$ (Nordion, Kanata, ON) mixed with 1.0 mol/L sodium acetate, pH 6.0, for 1 h at RT (Fig. 1). ^{111}In-labeled immunoconjugates were purified from free ^{111}In on an Amicon Ultra 30 K device. The radiochemical purity of the purified ^{111}In-labeled immunoconjugates was measured by instant thin layer-silica gel chromatography (ITLC-SG; Pall Life Sciences, Ann Arbor, MI) in 100 mM sodium citrate buffer, pH 5.0 (11). The SA achievable for labeling 2, 5 or 20 μg of immunoconjugates with 60 MBq of $^{111}InCl_3$ was determined.

HER2 Immunoreactivity

HER2 immunoreactivity of the immunoconjugates was evaluated by a competitive cell-binding assay. Approximately 2×10^5 SK-Br-3 cells were seeded into wells of 24-well plates (Sarstedt, Montreal, QC) and cultured for 24 h. The cells were then rinsed once with PBS, pH 7.5 and incubated with 10 nmol/L of ^{111}In-labeled DTPA-NLS-trastuzumab, DTPA-G4-trastuzumab or DTPA-G4-NLS-trastuzumab in the presence of trastuzumab (0–300 nmol/L) in 300 μL PBS (pH 7.5) containing 0.1% bovine serum albumin (BSA) at 4°C for 3.5 h. The cells were then rinsed with PBS and solubilized in 100 mmol/L NaOH. The dissolved cells were collected and the radioactivity was measured in a γ-counter (PerkinElmer Wizard 3, Wellesley, MA). The amount of ^{111}In-labeled immunoconjugates bound to SK-Br-3 cells was plotted *vs.* the increasing concentrations of trastuzumab and the resulting curve was fitted to a one site competition binding model using Prism Ver. 4.0 software (GraphPad, San Diego, CA). The effective concentration for displacement of 50% of the binding (EC_{50}) to SK-Br-3 cells was determined.

Internalization and Nuclear Importation

The internalization and nuclear importation of ^{111}In-labeled DTPA-G4-trastuzumab and DTPA-G4-NLS-trastuzumab in SK-Br-3 or MDA-MB-231 cells were measured by subcellular fractionation as previously reported (19). Briefly, 1×10^6 SK-Br-3 or 6×10^5 MDA-MB-231 cells were cultured overnight in wells in six-well plates and then blocked for 1 h with 3% BSA at RT. Then, ^{111}In-labeled DTPA-G4-trastuzumab or DTPA-G4-NLS-trastuzumab

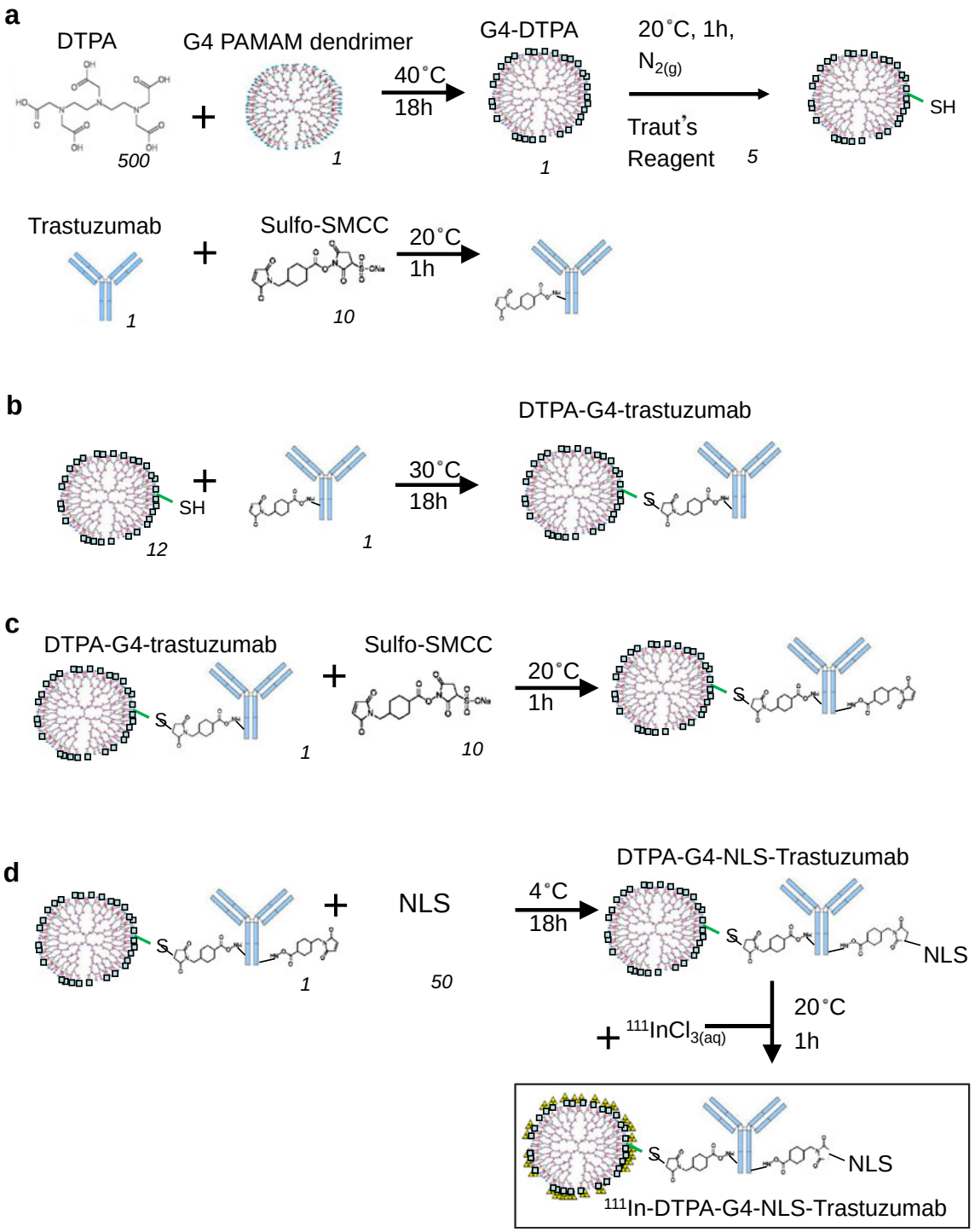

Fig. 1 Synthesis of ^{111}In-DTPA-G4-trastuzumab radioimmunoconjugates. (**a**) The surface amines on a G4 PAMAM dendrimer were modified with DTPA then with Traut's reagent (2-iminithiolane) to introduce a thiol. Maleimide groups were introduced into trastuzumab by reaction with Sulfo-SMCC. (**b**) DTPA-G4 with a free thiol was conjugated to maleimide-derivatized trastuzumab. (**c**) For conjugation to NLS peptides DTPA-G4-trastuzumab was further modified with Sulfo-SMCC to introduce a maleimide group. (**d**) NLS peptides [CGYGPKKKRKVGG] were introduced by reaction of maleimide-trastuzumab with the terminal cysteine on the peptides. Finally, DTPA-G4-trastuzumab with/without NLS was labeled to high specific SA with ^{111}In. The relative mole amounts in each of the above reactions are shown in italics.

(SA = 0.3 MBq/μg; 16.6 nmol/L) in 2 mL of growth medium (without FBS) containing 0.1% BSA, with or without a 50-fold excess of trastuzumab (830 nmol/L) was added to the wells. The dishes were incubated at 37°C for 4 h. The

medium was removed and the cells were rinsed once with 150 mM NaCl. Surface-bound radioactivity was displaced by incubation with 1 mL of 200 mmol/L Na acetate/500 mmol/L NaCl, pH 2.5, for 10 mins at RT. This was repeated once, and the acidic solutions were combined and collected (cell-membrane-bound fraction). Approximately 1 mL of ice-cold lysis buffer from the Nuclei Isolation Kit (NUC-101, Sigma-Aldrich) was then added to each well and incubated for 22 mins on ice. The lysed cells were collected. Each well was washed once more with nuclei lysis buffer and incubated for another 5 min. The recovered lysis buffer was centrifuged at 3000×g for 5 mins to separate the supernatant (cytoplasmic fraction) from the pellet (nuclei). Previous studies showed that this method provided good separation of cytoplasmic and nuclear fractions (20). The radioactivity in each fraction was measured in a γ-counter.

Clonogenic Survival and DNA DSBs

The effect of exposure to DTPA-G4-trastuzumab or DTPA-G4-NLS-trastuzumab labeled to high SA (5.9 MBq/μg; 8.7×10^5 MBq/μmole) on the clonogenic survival (CS) of SK-Br-3 or MDA-MB-231 cells was compared to low SA ^{111}In-DTPA-NLS-trastuzumab (0.5 MBq/μg; 7.4×10^4 MBq/μmole). Approximately 1.8×10^4 SK-Br-3 cells or 8×10^3 MDA-MB-231 cells were cultured overnight in wells in 96-well plates and then incubated with ^{111}In-labeled immunoconjugates (14 nmol/L) in growth medium without FBS at 37°C for 18 h. Controls consisted of cells cultured with growth medium alone, medium containing unlabeled DTPA-G4-NLS-trastuzumab, or ^{111}In-labeled DTPA-G4-NLS-IgG irrelevant (non-HER2 binding) immunoconjugates (5.9 MBq/μg; 8.7×10^5 MBq/μmole). Cells were rinsed with PBS, trypsinized, and 1.5×10^3 SK-Br-3 or 8×10^2 MDA-MB-231 cells were seeded in triplicate into T25 flasks and cultured for 14 d or 5 d, respectively. This period was adequate for colony formation (about 5 times the doubling times of SK-Br-3 and MDA-MB-231 cells) while avoiding confluence in T25 flasks. Surviving colonies were stained with methylene blue and colonies containing ≥50 cells counted. The CS was calculated by dividing the number of surviving colonies for treated cells by that for untreated cells. Cells were examined for foci of phosphorylated histone-2AX accumulation representing sites of unrepaired DNA double strand breaks (DSBs) by confocal immunofluorescence microscopy (γ-H2AX assay) (21).

Statistical Analysis

Data are presented as mean ± SD. Statistical analyses were performed with an unpaired *t*-test using Prism Ver 4.0 software (GraphPad Software Inc., San Diego, CA). $p<0.05$ was considered significant.

RESULTS

DTPA-G4-Trastuzumab and DTPA-G4-NLS-Trastuzumab

Based on preliminary studies (Fig. 2), a mole reaction ratio of 500:1 of DTPA:G4 dendrimer was chosen. This yielded approximately 30 DTPA chelators per dendrimer ($n=5$) and a modest increase in size (25 kDa) of the G4-trastuzumab immunoconjugates. Under these conditions, SDS-PAGE showed that DTPA-G4-trastuzumab migrated as two major bands corresponding to proteins with M_r of 205 kDa and 230 kDa (Lane 3, Fig. 3), respectively, and a very minor band at M_r of 180 kDa representing unmodified trastuzumab. These increases in M_r values for the immunoconjugates compared to trastuzumab (Lane 2, Fig. 3) were consistent with conjugation to one or two G4 dendrimers modified with 30 DTPA each. When DTPA-G4-trastuzumab was further reacted with a 10-fold mole excess of sulfo-SMCC cross-linker and then with a 50-fold mole excess of NLS peptides, there was an increase in M_r from 205 to 212 kDa and 230 to 235 kDa for the two bands (Lane 4, Fig. 3) corresponding to substitution with 3–4 NLS peptides per molecule.

Radiolabeling of Immunoconjugates

DTPA-G4-trastuzumab and DTPA-G4-NLS-trastuzumab (2, 5 or 20 μg) were labeled with ^{111}In to a SA of 23.6±0.9, 6.0±0.1 and 1.5±0.1 MBq/μg ($3.5\pm0.1\times10^6$, $0.9\pm0.2\times10^6$ and $0.2\pm0.01\times10^6$ MBq/μmole), respectively ($n=3$). DTPA-NLS-trastuzumab was labeled with ^{111}In to a SA of 0.5±0.1 MBq/μg, ($7.4\pm1.5\times10^4$ MBq/μmole). Following purification, the radiochemical purity of all immunoconjugates was 97.8±1.9% ($n=6$).

HER2 Immunoreactivity

The binding of ^{111}In-labeled DTPA-NLS-trastuzumab, DTPA-G4-trastuzumab and DTPA-G4-NLS-trastuzumab to HER2 on SK-Br-3 cells was displaced by increasing concentrations of trastuzumab (Fig. 4). The EC_{50} values for displacement of the binding of ^{111}In-labeled DTPA-NLS-trastuzumab, DTPA-G4-trastuzumab and DTPA-G4-NLS-trastuzumab were 1.7±0.2, 1.5±0.4 and 3.5±0.5 nmol/L, respectively. These EC_{50} values were significantly different ($p<0.05$) but the differences were <3-fold.

Internalization and Nuclear Importation

The internalization and nuclear importation of ^{111}In-labeled DTPA-G4-trastuzumab and DTPA-G4-NLS-trastuzumab were compared in SK-Br-3 and MDA-MB-231 cells (Fig. 5). The proportion of radioactivity that was cell-associated for

SK-Br-3 cells with respect to the total amount applied, was 0.6±0.2% and 0.6±0.1% for ^{111}In-labeled DTPA-G4-trastuzumab and DTPA-G4-NLS-trastuzumab, respectively. The percentage of cell-associated radioactivity for ^{111}In-labeled DTPA-G4-trastuzumab and DTPA-G4-NLS-trastuzumab that was internalized into SK-Br-3 cells after 4 h incubation at 37°C was 61.2±8.3% and 64.5±9.2% respectively ($p>0.05$; Fig. 5a). In the presence of excess trastuzumab, the internalization of ^{111}In-labeled DTPA-G4-trastuzumab and DTPA-G4-NLS-trastuzumab was reduced to 14.1±1.7% and 16.8±3.8%, respectively ($P<0.05$). This proportion of internalization was similar to that for MDA-MB-231 cells with or without HER2 blocking (Fig. 5a).

Nuclear importation of internalized radioactivity for ^{111}In-labeled DTPA-G4-trastuzumab and DTPA-G4-NLS-trastuzumab in SK-Br-3 cells was 52.9±9.0% and 56.0±9.3% ($p>0.05$), respectively (Fig. 5b). Nuclear importation was reduced to 8.6±1.4 and 10.1±3.0% with HER2 blocking ($P<0.0001$). A lower proportion of nuclear localization was observed for MDA-MB-231 cells and there were no significant differences between HER2 blocked and unblocked cells (8.5±2.2 and 9.9±4.0% *vs.* 9.5±3.3 and 11.4±4.8% for ^{111}In-labeled DTPA-G4-trastuzumab and DTPA-G4-NLS-trastuzumab, respectively; $p>0.05$).

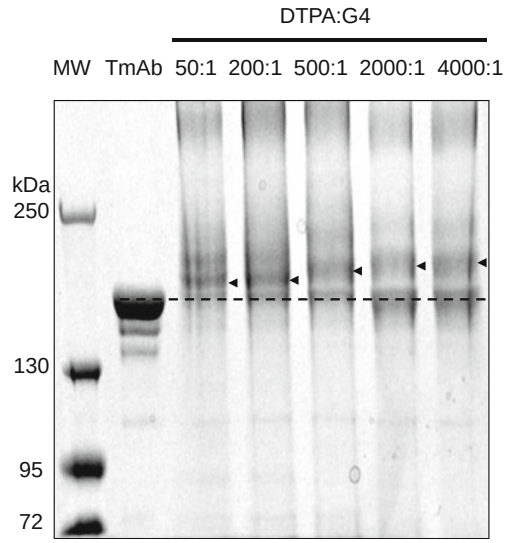

Fig. 2 SDS-PAGE analysis under non-reducing conditions on a 5% Tris HCl mini-gel stained with Coomassie Brilliant Blue of trastuzumab (TmAb) and DTPA-G4-trastuzumab synthesized using increasing mole ratios (shown) of DTPA:G4 PAMAM dendrimers. The upward shift in the bands for DTPA-G4-trastuzumab (*arrowheads*) compared to trastuzumab (*broken line*) was measured and used to estimate the number of DTPA conjugated to each dendrimer since the conditions for reaction of G4 dendrimers with trastuzumab were maintained constant for each mole ratio. Molecular weight markers are also shown (lane MW).

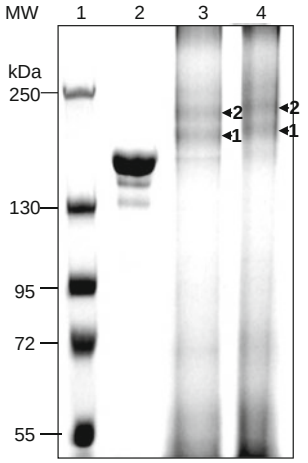

Fig. 3 SDS-PAGE analysis under non-reducing conditions on a 5% Tris HCl mini-gel stained with Coomassie Brilliant Blue of trastuzumab (lane 2), DTPA-G4-trastuzumab (lane 3) and DTPA-G4-NLS-trastuzumab (lane 4). Molecular weight markers are also shown (lane 1). Conjugation of trastuzumab to DTPA-modified G4 PAMAM dendrimers resulted in two bands (*arrowheads* 1 and 2). These bands likely represent trastuzumab modified with one or two G4 dendrimers derivatized with 30 DTPA chelators each.

Clonogenic Survival and DNA Double Strand Breaks

High SA ^{111}In-labeled G4 immunoconjugates (5.9 MBq/μg; 8.7×10^5 MBq/umole) were compared to low SA ^{111}In-DTPA-NLS-trastuzumab (0.5 MBq/μg; 7.4×10^4 MBq/umole) for decreasing the CS of SK-Br-3 cells with high HER2 density (Fig. 6a). The CS of SK-Br-3 cells was decreased to 11.3±7.0% and 16.1±7.3% with exposure to ^{111}In-DTPA-G4-trastuzumab or ^{111}In-DTPA-G4-NLS-

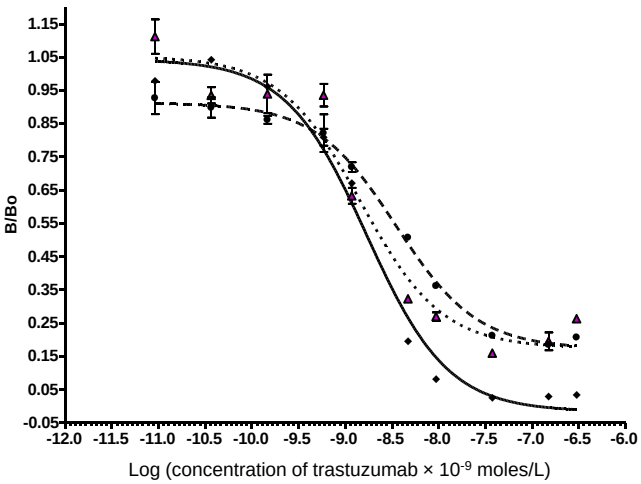

Fig. 4 Competition binding curve showing displacement of the binding of ^{111}In-DTPA-NLS-trastuzumab (♦), ^{111}In-DTPA-G4-trastuzumab (▲) or ^{111}In-DTPA-G4-NLS-trastuzumab (•) to SK-Br-3 cells (1.3×10^6 HER2/cell) by increasing concentrations of trastuzumab. EC_{50} values determined for these immunoconjugates were 1.7×10^{-9}, 1.5×10^{-9} and 3.5×10^{-9} mols/L, respectively. B/Bo = radioactivity bound in the presence of trastuzumab divided by radioactivity bound in the absence of trastuzumab.

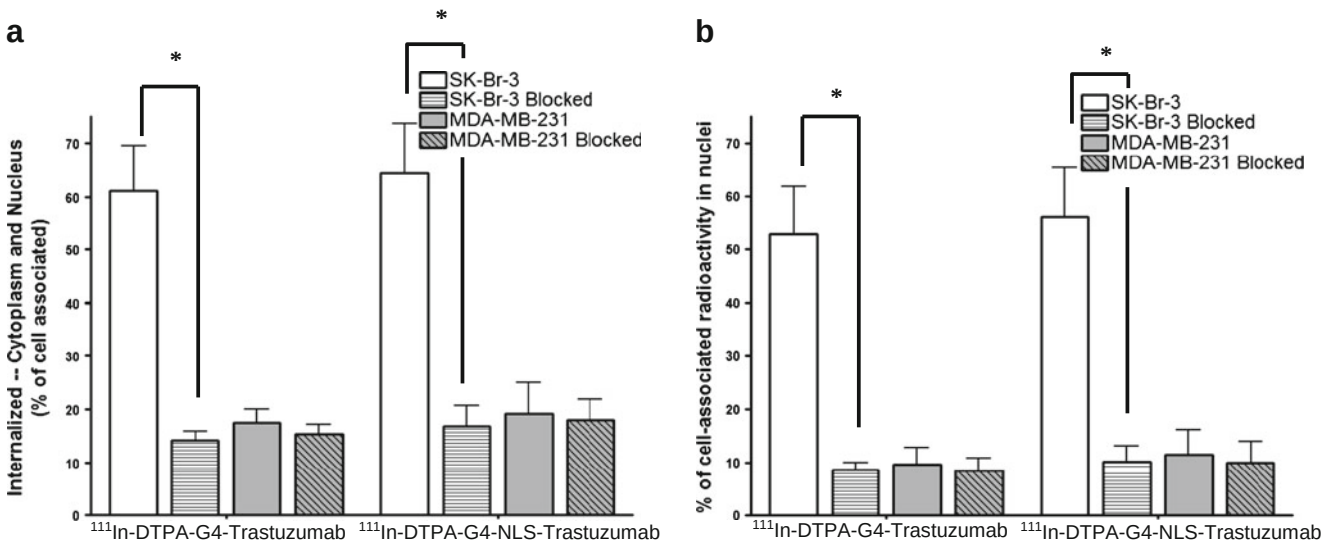

Fig. 5 Percentage of cell-associated radioactivity that was (**a**) internalized or (**b**) imported into the nucleus of SK-Br-3 cells with high HER2 density (1.3×10^6 receptors/cell) or MDA-MB-231 cells with low HER2 expression (2.8×10^4 receptors/cell) following incubation for 4 h at 37°C with ^{111}In-DTPA-G4-trastuzumab or ^{111}In-DTPA-G4-NLS-trastuzumab. Also shown is the internalized and nuclear radioactivity in the presence of excess trastuzumab to block HER2 receptors. Values shown are mean ± SD ($n = 4$–5). * Significantly different ($p < 0.05$).

trastuzumab, respectively ($p > 0.05$). These reductions in CS corresponded to a 3.7 and 2.6-fold increased cytotoxic potency, respectively for ^{111}In-DTPA-G4-trastuzumab and ^{111}In-DTPA-G4-NLS-trastuzumab compared to ^{111}In-DTPA-NLS-trastuzumab ($p < 0.001$). There was a 4-5 fold higher density of γ-H2AX foci in the nucleus of SK-Br-3 cells exposed to ^{111}In-DTPA-G4-trastuzumab or ^{111}In-DTPA-G4-NLS-trastuzumab, respectively, representing sites of unrepaired DNA DSBs (5.7±0.3 and 6.2±1.1, respectively, Fig. 7a and b) than in cells exposed to ^{111}In-DTPA-NLS-trastuzumab (1.3 ±0.2; $p < 0.001$). When SK-Br-3 cells were exposed to irrelevant ^{111}In-DTPA-G4-NLS-IgG, the CS was 56.4± 17.7% which was significantly greater than exposure to ^{111}In-DTPA-G4-trastuzumab or ^{111}In-DTPA-G4-NLS-trastuzumab ($p < 0.0001$).

The CS of MDA-MB-231 cells exposed to ^{111}In-DTPA-G4-trastuzumab or ^{111}In-DTPA-G4-NLS-trastuzumab was 7.0±4.1% and 7.2±3.4% respectively (Fig. 6b) which was 9.1–9.3 fold significantly lower than the CS for exposure to ^{111}In-DTPA-NLS-trastuzumab (68.4±17.7%; $p < 0.0001$). The integrated density of γ-H2AX foci representing sites of unrepaired DNA DSBs in MDA-MB-231 cells exposed to

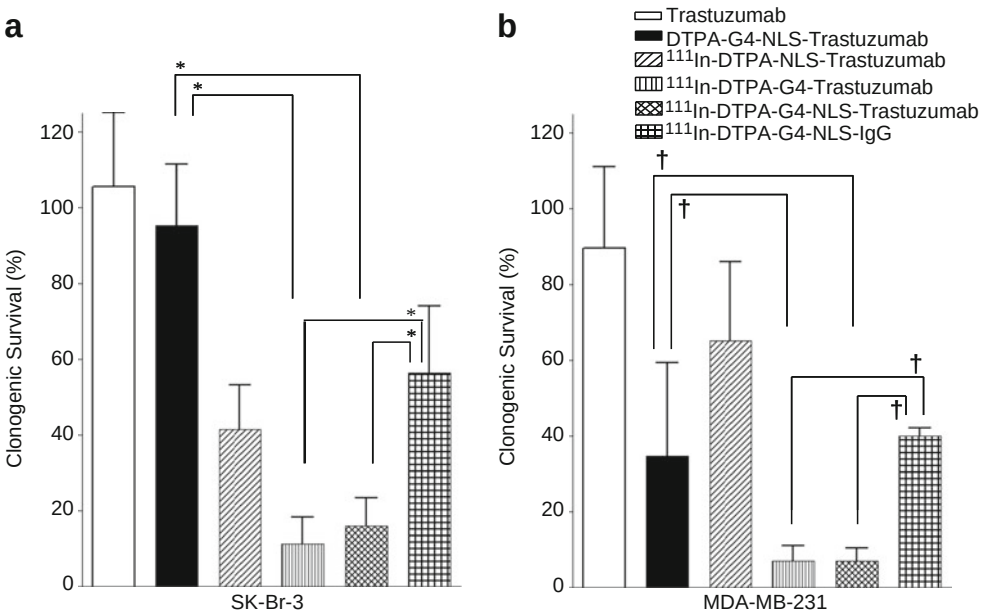

Fig. 6 Effect of exposure to 14 nmol/L of trastuzumab, unlabeled DTPA-G4-immunoconjugates or ^{111}In-DTPA-G4-immunoconjugates for 18 h then culturing for 14 d (SK-Br-3 cells) or 5 d (MDA-MB-231 cells) on clonogenic survival (CS). (**a**) SK-Br-3 cells overexpressing HER2 (1.3×10^6 receptors/cell). (**b**) MDA-MB-231 cells with low HER2 density (2.8×10^4 receptors/cell). The SA of ^{111}In-DTPA-G4-immunoconjugates was 5.9 MBq/μg (8.7×10^5 MBq/μmole) and ^{111}In-DTPA-NLS-trastuzumab was 0.5 MBq/μg (7.4×10^4 MBq/μmole). * Significantly different ($p < 0.0001$). † Significantly different ($p < 0.01$).

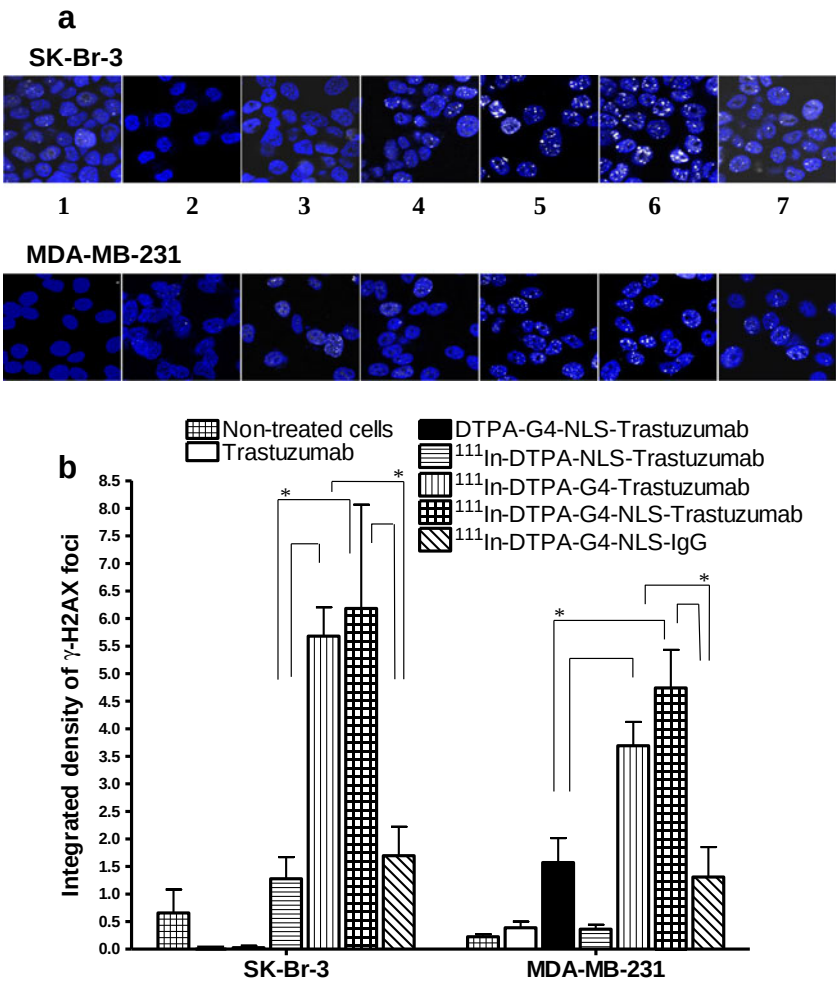

Fig. 7 (**a**) Unrepaired DNA DSBs visualized by immunofluorescence for γ-H2AX (bright foci) in SK-Br-3 (*top panel*) or MDA-MB-231 cells (*bottom panel*) treated with 1: growth medium, 2: trastuzumab, 3: unlabeled DTPA-G4-NLS-trastuzumab, 4: ^{111}In-DTPA-NLS-trastuzumab, 5: ^{111}In-DTPA-G4-trastuzumab, 6: ^{111}In-DTPA-G4-NLS-trastuzumab, 7: ^{111}In-DTPA-G4-NLS-IgG. The SA of ^{111}In-DTPA-NLS-trastuzumab was 0.5 MBq/μg (7.4×10^4 MBq/μmole) and ^{111}In-labeled DTPA-G4-immunoconjugates was 5.9 MBq/μg (8.7×10^5 MBq/μmole). Cells were incubated with 14 nmol/L of trastuzumab or immunoconjugates for 18 h at 37 °C. Nuclei were counterstained blue with 4,6-diamidino-2-phenylindole (DAPI). (**b**) Fold increase of integrated density of γ-H2AX foci in SK-Br-3 or MDA-MB-231 cells following these treatments. * Significantly different ($p < 0.05$).

^{111}In-DTPA-G4-trastuzumab (3.7±0.2) or ^{111}In-DTPA-G4-NLS-trastuzunab (4.7±0.4) was 10–13 fold significantly higher than for cells exposed to ^{111}In-DTPA-NLS-trastuzumab (0.4±0.1; $p<0.0001$; Fig. 7a and b). When MDA-MB-231 cells were exposed to ^{111}In-DTPA-G4-NLS-IgG, the CS was 40.0±2.2% (Fig. 6b). This was 6-fold significantly greater than exposure to ^{111}In-DTPA-G4-trastuzumab or ^{111}In-DTPA-G4-NLS-trastuzumab ($p=0.0033$ and 0.0016, respectively). The CS of MDA-MB-231 cells exposed to unlabeled DTPA-G4-NLS-trastuzumab was 34.7± 24.7% (Fig. 6b) which was significantly greater than exposure to ^{111}In-DTPA-G4-trastuzumab or ^{111}In-DTPA-G4-NLS-trastuzumab ($p=0.0200$ and 0.0123, respectively).

DISCUSSION

G4 PAMAM dendrimers were modified with multiple DTPA chelators for complexing ^{111}In by reaction with a 500-fold mole excess of DTPA dianhydride. Thiol groups were then introduced into DTPA-G4 for conjugation to maleimide-modified trastuzumab (Fig. 1). The increase in M_r observed by SDS-PAGE analysis (25 to 50 kDa; Fig. 3) was consistent with conjugation of trastuzumab to one or two G4 dendrimers derivatized with 30 DTPA each (expected M_r increase=26 kDa to 52 kDa). The number of thiols introduced into the G4 dendrimers was not measured but the mole ratio of thiolated G4:maleimide modified trastuzumab was 12:1 which would strongly favour monosubstitution of the G4 dendrimer with trastuzumab due to trastuzumab being in limiting amounts. Kobayashi *et al.* used an analogous approach involving reaction of G4 PAMAM dendrimers with a 50-fold mole excess of 2-(para-isothiocyanatobenzyl)-6-methyl-DTPS (IB4M) to introduce 43 IB4M chelators for complexing ^{111}In per dendrimer (18). They also introduced a thiol into IB4M-G4 dendrimers for conjugation to maleimide-modified OST7 murine IgG_1 antibodies. This resulted in a modest increase in M_r of the immunoconjugates (not quantified). DTPA dianhydride contains two functional groups reactive with amines on the G4 dendrimer in contrast to IB4M which presents one reactive isothiocyanate group, but G4 PAMAM dendrimers were not likely cross-linked through DTPA prior to conjugation to trastuzumab since this would result in greater

increases in M_r than were observed for the G4 immunoconjugates. Additional modification of G4 trastuzumab immunoconjugates to introduce NLS peptides increased the M_r by 5 to 7 kDa (Fig. 3) corresponding to 3–4 NLS peptides (M_r = 1.8 kDa each) per molecule. The NLS peptides may be conjugated through trastuzumab or the G4 dendrimers.

G4 trastuzumab immunoconjugates were labeled with ^{111}In to a SA that was up to 100-fold higher (23.6 MBq/μg; 3.5×10^6 MBq/μmole) than previously reported by our group for ^{111}In-DTPA-trastuzumab or ^{111}In-DTPA-NLS-trastuzumab (0.24 MBq/μg; 3.6×10^4 MBq/μmole) (6). Kobayashi *et al.* reported that IB4M-G4 PAMAM dendrimer conjugation to OST7 antibodies increased the SA for ^{111}In labeling by 54-fold from 8.7 MBq/μg (1.3×10^6 MBq/μmole) to 470 MBq/μg (7.0×10^7 MBq/μmole) (18). G4 trastuzumab immunoconjugates retained HER2 immunoreactivity as evidenced by the similar EC_{50} values for displacement of the binding of ^{111}In-DTPA-G4-trastuzumab, ^{111}In-DTPA-G4-NLS-trastuzumab or ^{111}In-DTPA-NLS-trastuzumab to SK-Br-3 cells by trastuzumab (Fig. 4). Wängler *et al.* noted that the number of PAMAM dendrimers conjugated to hMAb425 antibodies was the most important factor effecting immunoreactivity with 62.7% immunoreactivity at 1.7 dendrimers per antibody decreasing to 17.1% at 10 dendrimers per antibody (22). The low G4 dendrimer substitution level in our study (1 or 2 dendrimers/antibody) preserved the HER2 immunoreactivity. Kobayashi *et al.* found only minimal changes in the immunoreactivity of OST7 antibodies modified with IB4M-G4 dendrimers (18). Others have similarly reported preserved immunoreactivity of antibodies modified with dendrimers (13–15).

Approximately 60–65% of cell-bound radioactivity was internalized within 4 h at 37°C following incubation of SK-Br-3 cells with ^{111}In-DTPA-G4-trastuzumab or ^{111}In-DTPA-G4-NLS-trastuzumab (Fig. 5). The proportion of internalized radioactivity in SK-Br-3 cells was 1.5-fold higher than previously found for ^{111}In-DTPA-NLS-trastuzumab (~40%) (6). Internalization was HER2-mediated however since it was decreased 4-fold by blocking HER2 on SK-Br-3 cells with excess trastuzumab. Nonetheless, conjugation of trastuzumab to G4 PAMAM dendrimers may promote internalization. Shukla *et al.* found that G5 PAMAM dendrimers conjugated to HER2 antibodies enhanced the delivery of AlexaFluor dye into SK-Br-3 cells (14). Miyano *et al.* reported increased internalization in SK-Br-3 cells when trastuzumab was modified with a G6 lysine dendrimer (23). Nuclear importation of ^{111}In-DTPA-G4-trastuzumab and ^{111}In-DTPA-G4-NLS-trastuzumab was efficient with about 50% of the internalized radioactivity found in the nucleus. Unexpectedly, there was no significant increase in nuclear localization of ^{111}In-DTPA-G4-trastuzumab in SK-Br-3 cells with NLS peptide modification in contrast to our previous studies comparing ^{111}In-DTPA-trastuzumab and ^{111}In-NLS-trastuzumab (6). It is possible that the cationic charges on G4 dendrimers obviate the need for NLS peptide modification of trastuzumab since nuclear importation is thought to be enabled by sequences of cationic amino acids (*e.g.* lysine or arginine) on these peptides which interact with importins (24). Kang *et al.* found that cationic TAT peptides conjugated to G5 PAMAM dendrimers and complexed to antisense or siRNA oligodeoxnucleotides did not improve internalization or nuclear delivery compared to the unmodified dendrimer complexes (25). HER2 likely also plays an important role in routing the G4 trastuzumab radioimmunoconjugates to the nucleus since nuclear uptake was 5-fold lower in MDA-MB-231 cells (5.4×10^4 receptors/cell) than in SK-Br-3 cells (1.3×10^6 receptors/cell; Fig. 5). Moreover, HER2 harbours a putative NLS in the transmembrane domain of the receptor which may facilitate nuclear importation (26). Cellular radiation dosimetry modeling by our group using Monte Carlo N-Particle (MCNP) computer code has revealed that the radiation absorbed dose deposited in the nucleus of SK-Br-3 human cells is 6-fold higher when ^{111}In was deposited in the nucleus compared to the cytoplasm, and 15-fold higher than when ^{111}In was located on the cell surface (27). Thus, it is important to deliver ^{111}In into the cell nucleus to maximize the lethal DNA damaging effects of the Auger electrons.

High SA ^{111}In-labeled DTPA-G4-trastuzumab and DTPA-G4-NLS-trastuzumab immunoconjugates (5.9 MBq/μg; 8.7×10^5 MBq/μmole) were 2–4 fold more potent than low SA ^{111}In-DTPA-NLS-trastuzumab (0.5 MBq/μg; 7.4×10^4 MBq/μmole) at reducing the CS of SK-Br-3 cells with high HER2 density (1.3×10^6 receptors/cell; Fig. 6a). This increased potency was associated with a 4–5 fold greater density of γ-H2AX foci in the nucleus of SK-Br-3 cells, representing sites of unrepaired DNA DSBs (Fig. 7). Moreover, ^{111}In-DTPA-G4-trastuzumab and ^{111}In-DTPA-G4-NLS-trastuzumab were 9-fold more effective than ^{111}In-DTPA-NLS-trastuzumab at decreasing the CS of MDA-MB-231 cells with low HER2 density (5.4×10^4 receptors/cell; Fig. 6b). The increased potency towards MDA-MB-231 cells was associated with a 10–13 fold greater density of DNA DSBs (Fig. 7). These results confirm our previous report that MDA-MB-231 cells were relatively resistant to ^{111}In-DTPA-NLS-trastuzumab due to low HER2 density (6) but for the first time we now reveal that high SA ^{111}In-labeled G4-trastuzumab radioimmunoconjugates can overcome this resistance. ^{111}In-DTPA-G4-NLS-IgG irrelevent immunoconjugates (non HER2-binding) were also cytotoxic to SK-Br-3 and MDA-MB-231 cells but were 3.5 and 5.6-fold significantly less potent ($p < 0.002$) than G4-trastuzumab radioimmunoconjugates (Fig. 6). In addition, the density of DNA DSBs was lower in SK-Br-3 and MDA-MB-231 cells exposed to ^{111}In-DTPA-G4-NLS-IgG

(Fig. 7). These findings indicated that ^{111}In-DTPA-G4-trastuzumab and ^{111}In-DTPA-G4-NLS-trastuzumab exhibited HER2-mediated cytotoxicity but there may also be some non-HER2 mediated toxic effects, possibly due to the longer range γ-emissions of ^{111}In or the chemical toxicity of G4 dendrimers (28). The possibility of G4-mediated toxicity was suggested by the decreased CS of MDA-MB-231 cells when exposed to unlabeled DTPA-G4-NLS-trastuzumab (Fig. 6b). However, there was no toxicity of unlabeled DTPA-G4-NLS-trastuzumab on SK-Br-3 cells (Fig. 6a), suggesting that these effects are more important for cells that have low HER2 density. The toxicity of G4 dendrimers may be due to the positive charges which cause binding to negatively-charged cell membranes (29). Dendrimer-mediated cytotoxicity may be mediated by cell membrane damage and hole formation (28). In our study, the G4 dendrimers conjugated to trastuzumab had 30 of 64 surface amines modified with DTPA and one amine modified with 2-iminothiolane to introduce a thiol for conjugation to trastuzumab. These modifications reduced the number of positive charges by 2-fold. Furthermore, ^{111}In-labeling of DTPA chelators on the G4 dendrimers results in a net charge of (−1) for these complexes. These negative charges may counteract the positive charges on the remaining unmodified amines on G4 dendrimers. It is also possible that the high number of DTPA groups on the G4 dendrimers contributed to the cytotoxicity of unlabeled DTPA-G4-trastuzumab on MDA-MB-231 cells since DTPA has been shown to be cytotoxic due to complexing Ca^{2+} or Zn^{2+} ions (30, 31). However, these cytotoxic concentrations of DTPA were 700-fold to 7,000-fold higher than employed in our study, suggesting that the cytotoxicity of unlabeled DTPA-G4-trastuzumab may be mediated mostly by the G4 dendrimer.

CONCLUSIONS

We conclude that conjugation of trastuzumab to G4 PAMAM dendrimers derivatized with 30 DTPA groups retained HER2 immunoreactivity and permitted labeling with ^{111}In up to 100-fold higher SA than ^{111}In-DTPA-NLS-trastuzumab. The higher SA of these ^{111}In-labeled G4 immunoconjugates resulted in increased potency than ^{111}In-DTPA-NLS-trastuzumab for reducing the CS of human BC cells with high or low HER2 density which was associated with a greater density of unrepaired DNA DSBs.

ACKNOWLEDGMENTS AND DISCLOSURES

The authors gratefully acknowledge financial support from the Canadian Breast Cancer Research Alliance (Grant 019513) with funds from the Canadian Cancer Society. Parts of this study were presented at the Annual Congress of the European Association of Nuclear Medicine in Birmingham, U.K. October 15 to 19, 2011.

REFERENCES

1. Revillion F, Bonneterre J, Peyrat JP. ERBB2 oncogene in human breast cancer and its clinical significance. Eur J Cancer. 1998;34:791–808.
2. Vogel CL, Cobleigh MA, Tripathy D, Gutheil JC, Harris LN, Fehrenbacher L, *et al.* Efficacy and safety of trastuzumab as a single agent in first-line treatment of HER2-overexpressing metastatic breast cancer. J Clin Oncol. 2002;20:719–26.
3. Slamon DJ, Leyland-Jones B, Shak S, Fuchs H, Paton V, Bajamonde A, *et al.* Use of chemotherapy plus a monoclonal antibody against HER2 for metastatic breast cancer that overexpresses HER2. N Engl J Med. 2001;344:783–92.
4. Cobleigh MA, Vogel CL, Tripathy D, Robert NJ, Scholl S, *et al.* Multinational study of the efficacy and safety of humanized anti-HER2 monoclonal antibody in women who have HER2-overexpressing metastatic breast cancer that has progressed after chemotherapy for metastatic disease. J Clin Oncol. 1999;17:2639–48.
5. Tokunaga E, Oki E, Kojiro N, Koga T, Egashira A, *et al.* Trastuzumab and breast cancer: developments and current status. Int J Cin Oncol. 2006;11:199–208.
6. Costantini DL, Chan C, Cai Z, Vallis KA, Reilly RM. ^{111}In-labeled trastuzumab (Herceptin) modified with nuclear localizing sequences (NLS): An Auger electron-emitting radiotherapeutic agent for HER2/neu-amplified breast cancer. J Nucl Med. 2007;48:1357–68.
7. Kassis AI. Cancer therapy with Auger electrons: are we almost there? J Nucl Med. 2003;44:1479–81.
8. Yoneda Y, Arioka T, Imamoto-Sonobe N, Sugawa H, Shimonishi Y, Uchida T. Synthetic peptides containing a region of SV 40 large T-antigen involved in nuclear localization direct the transport of proteins into the nucleus. Exp Cell Res. 1987;170:439–52.
9. Costantini DL, McLarty K, Lee H, Done SJ, Vallis KA, Reilly RM. Antitumor effects and normal-tissue toxicity of ^{111}In-nuclear localization sequence-trastuzumab in athymic mice bearing HER-positive human breast cancer xenografts. J Nucl Med. 2010;51:1084–91.
10. Wolff AC, Hammond EH, Schwartz JN, Hagerty KL, Allred DC, *et al.* American society of clinical oncology/college of american pathologists guideline recommendations for human epidermal growth factor receptor 2 testing in breast cancer. J Clin Oncol. 2007;25:118–45.
11. Reilly RM. The radiochemistry of monoclonal antibodies and peptides. In: Reilly RM, editor. Monoclonal antibody and peptide-targeted radiotherapy of cancer. Hoboken: John Wiley & Sons; 2010. p. 39–100.
12. Boyle AJ, Liu P, Lu Y, Weinrich D, Scollard DA, Ngo Njock Mbong G, *et al.* The effect of metal-chelating polymers (MCPs) for ^{111}In complexed *via* the streptavidin-biotin system to trastuzumab Fab fragments on tumor and normal tissue distribution in mice. Pharm Res. 2013;30:104–16.
13. Wu G, Barth RF, Yang W, Kawabata S, Zhang L, Green-Church K. Targeted delivery of methotrexate to epidermal growth factor receptor-positive brain tumors by means of cetuximab (IMC-C225) dendrimer bioconjugates. Mol Cancer Ther. 2006;5:52–9.
14. Shukla R, Thomas TP, Peters JL, Desai AM, Kukowska-Latallo J, Patri AK, *et al.* HER2 specific tumor targeting with dendrimer conjugated anti-HER2 mAb. Bioconjug Chem. 2006;17:1109–15.
15. Wu G, Barth RF, Yang W, Chatterjee M, Tjarks W, Ciesielski MJ, *et al.* Site-specific conjugation of boron-containing dendrimers to anti-EGF receptor monoclonal antibody cetuximab (IMC-C225) and its evaluation as a potential delivery agent for neutron capture therapy. Bioconjug Chem. 2004;15:185–94.

16. Reilly RM, Kassis A. Targeted auger electron radiotherapy of malignancies. In: Reilly RM, editor. Monoclonal antibody and peptide-targeted radiotherapy of cancer. Hoboken: Wiley; 2010. p. 289–348.
17. McLarty K, Cornelissen B, Scollard DA, Done SJ, Chun K, Reilly RM. Associations between the uptake of ^{111}In-DTPA-trastuzumab, HER2 density and response to trastuzumab (Herceptin) in athymic mice bearing subcutaneous human tumour xenografts. Eur J Nucl Med Mol Imaging. 2009;36:81–93.
18. Kobayashi H, Sato N, Saga T, Nakamoto Y, Ishimori T, Toyama S, *et al.* Monoclonal antibody-dendrimer conjugates enable radiolabeling of antibody with markedly high specific activity with minimal loss of immunoreactivity. Eur J Nucl Med. 2000;27:1334–9.
19. Chan C, Cai Z, Su R, Reilly RM. ^{111}In- or ^{99m}Tc-labeled recombinant VEGF bioconjugates: *in vitro* evaluation of their cytotoxicity on porcine aortic endothelial cells overexpressing Flt-1 receptors. Nucl Med Biol. 2010;37:105–15.
20. Hu M, Chen P, Wang J, Chan C, Scollard DA, Reilly RM. Site-specific conjugation of HIV-1 tat peptides to IgG: a potential route to construct radioimmunoconjugates for targeting intracellular and nuclear epitopes in cancer. Eur J Nucl Med Mol Imaging. 2006;33:301–10.
21. Cai Z, Chen Z, Bailey KE, Scollard DA, Reilly RM, Vallis KA. Relationship between induction of phosphorylated H2AX and survival in breast cancer cells exposed to ^{111}In-DTPA-hEGF. J Nucl Med. 2008;49:1353–61.
22. Wängler C, Moldenhauer G, Eisenhut M, Haberkorn U, Mier W. Antibody-dendrimer conjugates: the number, not the size of the dendrimers, determines the immunoreactivity. Bioconjug Chem. 2008;19:813–20.
23. Miyano T, Wijagkanalan W, Kawakami S, Yamashita F, Hashida M. Anionic amino acid dendrimer-trastuzumab conjugates for specific internalization in HER2-positive cancer cells. Mol Pharm. 2010;7:1318–27.
24. Costantini DL, Hu M, Reilly RM. Peptide motifs for insertion of radiolabeled biomolecules into cells and routing to the nucleus for cancer imaging or radiotherapeutic applications. Cancer Biother Radiopharm. 2008;23:3–24.
25. Kang H, DeLong R, Fisher MH, Juliano RL. Tat-conjugated PAMAM dendrimers as delivery agents for antisense and siRNA oligonucleotides. Pharm Res. 2005;22:2099–106.
26. Chen QQ, Chen XY, Jiang YY, Liu J. Identification of novel nuclear localization signal within the ErbB-2 protein. Cell Res. 2005;15:504–10.
27. Cai Z, Pignol JP, Chan C, Reilly RM. Cellular dosimetry of ^{111}In using Monte Carlo N-particle computer code: comparison with analytic methods and correlation with *in vitro* cytotoxicit. J Nucl Med. 2010;51:462–70.
28. Duncan R, Izzo L. Dendrimer biocompatibility and toxicity. Adv Drug Deliv Rev. 2005;57:2215–37.
29. Malik N, Wiwattanapatapee R, Klopsch R, Lorenz K, Frey H, Weener JW, *et al.* Dendrimers: relationship between structure and biocompatibility *in vitro*, and preliminary studies on the biodistribution of ^{125}I-labelled polyamidoamine dendrimers *in vivo*. J Control Release. 2000;65:133–48.
30. Lücke-Huhle C. Proliferation-dependent cytotoxicity of diethylenetriaminepentaacetate (DTPA) *in vitro*. Health Phys. 1976;31:349–54.
31. Michaelis M, Langer K, Arnold S, Doerr HW, Kreuter J, Cinatl Jr J. Pharmacological activity of DTPA linked to protein-based drug carrier systems. Biochem Biophys Res Commun. 2004;323:1236–40.